# Synthesis, Characterization, Thermal Decomposition, and Kinetic Studies of Binuclear Sulfur-Coordinated Tungsten(V) Complexes with Piperidine-1-carbodithioate

by **Rafael Lozano***[a]), **Fernando de Jesús**[b]), **Mercedes Cano de Santayana**[c]), and **M. Carmen Lozano**[b])

[a]) Departamento de Química Inorgánica y Bioinorgánica, Facultad de Farmacia, Universidad Complutense, ES-28040 Madrid (phone: +34913941717; fax: +34913941705; e-mail: rlozano@farm.ucm.es)

[b]) Facultad de Farmacia, Universidad Alfonso X el Sabio, ES-28691 Villanueva de la Cañada (Madrid)

[c]) ICAI, Universidad Pontificia de Comillas, ES-28015 Madrid

We describe the synthesis, characterization by IR and electronic spectra, magnetic susceptibility measurements, analytical data, kinetic study by differential-scanning calorimetry, and thermogravimetric analysis of the thermal decomposition under $N_2$ of the adducts **2**–**7** with pyridine or substituted pyridines of bis(piperidine-1-carbodithioato-$\kappa S,\kappa S'$)di-$\mu$-thioxodithioxoditungsten(V) (**1**), to which the general formula $[W_2B_2(pipCS_2)_2S_2(\mu\text{-}S)_2]$ is assigned ($pipCS_2$ = piperidine-1-carbodithioato and B = pyridine (py), 3-methylpyridine (3-Mepy), 4-methylpyridine (4-Mepy), 3,5-dimethylpyridine (3,5-$Me_2$py), pyridin-3-amine (3-py$NH_2$), and pyridin-4-amine (4-py$NH_2$)). For the endothermic process of loss of the coordinated base B, we calculated activation energies with a method reported previously by us; the mechanism and pre-exponential *Arrhenius* factor of this reaction were also determined. A relationship between the pyridines' basicity, IR and electronic spectral data, and activation energies was established.

**Introduction.** – In contrast to the large amount of work which has centred on the chemistry of dimeric $Mo^V$ complexes with carbamodithioates, xanthates (=carbonodithioates), oxines (=quinolin-8-ols), *etc.* [1–6], much less attention has been drawn to the chemistry of dimeric $W^V$ complexes. However, we have reported the study and characterization of dimeric $W^V$ complexes with carbamates, xanthates, carbamodithioates, and oxines as ligands [7–14].

The relevance to the bioinorganic chemistry of Mo and W and also to heterogeneous catalysis has been stressed several times in the literature. Mo or W is present at the active sites of over 30 different enzymes. Several of these enzymes confirm the potential additional presence of oxo (one or two), thioxo, cysteine, selenocysteine, serine, aquo/hydroxo, and/or a second dithiolene in the various metal coordination spheres [15–20]. The relevance of Mo and W complexes in the bioinorganic processes is related to the force of union among them and the different ligands with which they react. For this reason, we establish a relationship between the basic force of different organic bases and the activation energies obtained for the processes of thermal decomposition of several adducts with pyridine or substituted pyridines of binuclear $W^V$ complexes.

In this article, we describe the syntheses by reactions in different solvents, characterization, and thermal decomposition of the bis(piperidine-1-carbodithioato-$\kappa S,\kappa S'$)di-$\mu$-thioxodithioxoditungsten(V) adducts **2**–**7** with pyridine or substituted

pyridines (3-methylpyridine (3-Mepy), 4-methylpyridine (4-Mepy), 3,5-dimethylpyridine (3,5-$Me_2$py), pyridin-3-amine (3-py$NH_2$), and pyridin-4-amine (4-py$NH_2$)) by direct reaction between the complex **1** and the pyridines and conversion of five- to six-coordinate metal centers. The study of the adducts **2**–**7** by IR and electronic spectroscopy, magnetic susceptibilities, and analytical data showed that the stoichiometry of the complex is 1:1 for the ligand metal ratio and 2:1 for the base/complex ratio.

The kinetic parameters and the reaction mechanism of the process studied were also shown in the *Scheme*. The activation energy and the pre-exponential *Arrhenius* factor for this process were determined with a nonisothermal kinetic method reported previously by us. The determination of kinetic parameters by nonisothermal methods offers interesting advantages over conventional isothermal studies [21–28]. Only a single sample and fewer data are required, and the kinetics can be calculated over an entire temperature range in a continuous manner. However, a disadvantage of the nonisothermal methods, as compared to the isothermal techniques, is that usually the reaction mechanism cannot be determined, and hence the meaning of the kinetics parameters is uncertain. With our method, the reaction mechanism can also be determined [29–31]. A comparison between the activation energies ($E_a$), steric or inductive factors, IR data, and p$K_b$ values of the coordinated bases in adducts **2**–**7** was also made.

*Scheme*

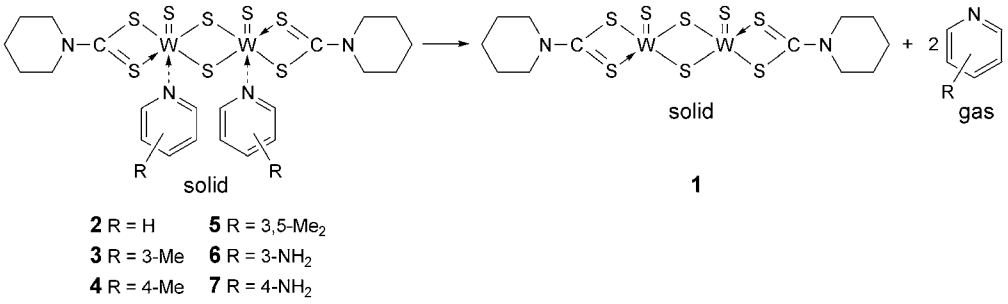


**Experimental.** – *General.* UV/VIS Spectra: *Beckman DU7* spectrophotometer; complex solns. in DMSO or $CH_2Cl_2$; measurements in the range 200–900 nm. IR Spectra: *Perkin-Elmer 283* spectrophotometer. Elemental analysis: *Perkin-Elmer 240-B* elemental analyzer; W was determined by atomic absorption with a *Perkin-Elmer 430* atomic absorption spectrophotometer, after decomposing the complexes with a 1:1 mixture of conc. $HNO_3$ soln. and $H_2SO_4$.

*Magnetic Susceptibilities. Mettler H-51-AR* Balance and type *C Newport* electromagnet; measurements by *Gouy*'s method at r.t., molar susceptibilities corrected for the diamagnetism of the constituent molecules [32].

*Thermogravimetric Measurements. Mettler TA-3000* system fitted with a *Mettler TG-50* thermobalance; $Al_2O_3$ pan; heating rate 2°/min; sample mass 5 mg; under dynamic $N_2$ up to 250° and then under air up to 600°.

*Differential-Scanning Calorimetry* (DSC): *Mettler TA-3000* system fitted with a *Mettler DSC-20* differential scanning calorimeter; aluminium pan; from 25 to 600° at a scanning rate of 2°/min; *ca.* 5 mg sample as very fine powder to render insignificant the nonuniform temp. within the sample; under

dynamic $N_2$ up to 250° and then under air up to 600°; periodical instrument calibration with standard samples of In (99.99 % purity); several runs were made in all cases.

*Syntheses. Bis(piperidine-1-carbodithioato-κS,κS′)di-μ-thioxodithioxoditungsten* ([$W_2$(pip$CS_2$)$_2$$S_2$(μ-S)$_2$]; formerly also [$W_2S_4$(piperidinedtc)$_2$]; **1**): Preparation as reported previously [11]. $\mu = 0.03$ B.M. Anal. calc.: W 45.08, C 17.65, H 2.45, N 3.43, S 31.38; found: W 45.19, C 17.01, H 2.54, N 3.66, S 31.39.

*Adducts [$W_2B_2$(pip$CS_2$)$_2$$S_2$(μ-S)$_2$]*. [$W_2$(pip$CS_2$)$_2$$S_2$(μ-S)$_2$] (**1**; 0.01 mol) was dissolved in 0.02 mol of pyridine or 3-methyl-, 4-methyl-, or 3,5-dimethylpyridine, or in an EtOH soln. of 0.02 mol of pyridin-3-amine or pyridin-4-amine, and heated in a water bath for *ca.* 15 min. After cooling for 3 days, the adducts **2**–**7** were obtained as brownish powders by filtration *in vacuo*, and dried over $P_4O_{10}$ under $N_2$.

*Bis(piperidine-1-carbodithioato-κS,κS′)bis(pyridine)di-μ-thioxodithioxoditungsten* ([$W_2$(pip$CS_2$)$_2$(py)$_2$$S_2$(μ-S)$_2$]; **2**): $\mu = 0.00$ B.M. Anal. calc.: W 37.76, C 27.11, H 3.08, N 5.75, S 26.29; found: W 37.02, C 27.23, H 3.04, N 5.76, S 26.34.

*Bis(3-methylpyridine)bis(piperidine-1-carbodithioato-κS,κS′)di-μ-thioxodithioxoditungsten* ([$W_2$(pip$CS_2$)$_2$(3-Mepy)$_2$$S_2$(μ-S)$_2$]; **3**): $\mu = 0.01$ B.M. Anal. calc.: W 36.71, C 28.75, H 3.39, N 5.59, S 25.56; found: W 36.99, C 29.02, H 3.35, N 5.42, S 25.54.

*Bis(4-methylpyridine)bis(piperidine-1-carbodithioato-κS,κS′)di-μ-thioxodithioxoditungsten* ([$W_2$(pip$CS_2$)$_2$(4-Mepy)$_2$$S_2$(μ-S)$_2$]; **4**): $\mu = 0.11$ B.M. Anal. calc.: W 36.71, C 28.75, H 3.39, N 5.59, S 25.56; found: W 37.03, C 28.77, H 3.32, N 5.53, S 25.52.

*Bis(3,5-dimethylpyridine)bis(piperidine-1-carbodithioato-κS,κS′)di-μ-thioxodithioxoditungsten* ([$W_2$(pip$CS_2$)$_2$(3,5-$Me_2$py)$S_2$(μ-S)$_2$]; **5**): $\mu = 0.07$ B.M. Anal. calc.: W 35.71, C 30.30, H 3.69, N 5.44, S 24.86; found: W 35.77, C 30.28, H 3.59, N 5.39, S 25.02.

*Bis(piperidine-1-carbodithioato-κS,κS′)bis(pyridin-3-amine-κN¹)di-μ-thioxodithioxoditungsten* ([$W_2$(pip$CS_2$)$_2$(3-py$NH_2$)$_2$$S_2$(μ-S)$_2$]; **6**): $\mu = 0.01$ B.M. Anal. calc.: W 36.63, C 26.30, H 3.19, N 8.37, S 25.51; found: W 36.72, C 26.38, H 3.14, N 8.34, S 25.53.

*Bis(piperidine-1-carbodithioato-κS,κS′)bis(pyridin-4-amine-κN¹)di-μ-thioxodithioxoditungsten* ([$W_2$(pip$CS_2$)$_2$(4-py$NH_2$)$_2$$S_2$(μ-S)$_2$]; **7**): $\mu = 0.00$ B.M. Anal. calc.: W 36.63, C 26.30, H 3.19, N 8.37, S 25.51; found: W 36.56, C 26.37, H 3.14, N 8.47, S 25.68.

*Kinetic Studies.* The rate of a thermal decomposition reaction of a solid can be expressed by the *Arrhenius* equation (*Eqn. 1*). In *Eqn. 1*, $\alpha$ is the fraction of material which reacts at time $t$, $E_a$ is the activation energy, $f(\alpha)$ is a function which depends on the actual reaction mechanism, and $A$ is the pre-exponential *Arrhenius* factor. *Table 1* summarizes the mathematical expressions of the functions $f(\alpha)$ corresponding to some of the thermal decomposition mechanisms found in the literature [27]. When the temperature of the sample is increased at a constant rate, we can write *Eqn. 2* where $\beta$ is the heating rate, $dT/dt$. By differentiating the logarithmic form of *Eqn. 2* with respect to $d\ln(1-\alpha)$, we obtain *Eqn. 3*. Thus, the plots of $[\Delta\ln\alpha' - \Delta\ln f(\alpha)]/\Delta\ln(1-\alpha)$ *vs.* $[\Delta(1/T)/\Delta\ln(1-\alpha)]$ should be a straight line with a slope $-E_a/R$, irrespective of the $f(\alpha)$ employed. However, we can select the $f(\alpha)$ that best fits the actual reaction mechanism studied, by means of the intercept value, which in ideal agreement with *Eqn. 3* should be zero.

$$d\alpha/dt = A e^{-E_a/RT} f(\alpha) \tag{1}$$

$$d\alpha/dT = \alpha' = (A/\beta) e^{-E_a/RT} f(\alpha) \tag{2}$$

$$d\ln\alpha'/d\ln(1-\alpha) = -(E_a/R)[d(1/T)/d\ln(1-\alpha)] + [d\ln f(\alpha)/d\ln(1-\alpha)]$$

or

$$\Delta\ln\alpha'/\Delta\ln(1-\alpha) = -(E_a/R)[\Delta(1/T)/\Delta\ln(1-\alpha)] + [\Delta\ln f(\alpha)/\Delta\ln(1-\alpha)]$$

and

$$[\Delta\ln\alpha' - \Delta\ln f(\alpha)]/\Delta\ln(1-\alpha) = -(E_a/R)[\Delta(1/T)/\Delta\ln(1-\alpha)] \tag{3}$$

To test the validity of the above conclusions, we have substituted the seven forms of $f(\alpha)$ into the *Arrhenius* equation in logarithmic form (*Eqn. 2*), giving *Eqn. 4*. The plot of $\ln\alpha' - \ln f(\alpha)$ *vs.* $1/T$ should

Table 1. *Kinetic Equations*

| Mechanism (rate-controlling process) | $f(\alpha)$ |
|---|---|
| *D*1 (one-dimensional diffusion) | $(1/2\alpha)$ |
| *D*2 (two-dimensional diffusion) | $[-\ln(1-\alpha)]^{-1}$ |
| *D*3 (three-dimensional diffusion: *Jander*'s equation) | $(3/2)(1-\alpha)^{2/3}[1-(1-\alpha)^{1/3}]^{-1}$ |
| *D*4 (three-dimensional diffusion: *Ginstling–Brounshtein* equation) | $(3/2)[(1-\alpha)^{-1/3}-1]^{-1}$ |
| *F*1 (random nucleation) | $(1-\alpha)$ |
| *R*2 (phase-boundary reaction: cylindrical symmetry) | $2(1-\alpha)^{1/2}$ |
| *R*3 (phase-boundary reaction: spherical symmetry) | $3(1-\alpha)^{2/3}$ |

be a straight line with a slope $-E_a/R$ and intercept $\ln(A/\beta)$. If the suggested mechanism is correct, the activation energy value should be the same as that obtained previously.

$$\ln\alpha' = \ln(A/\beta) - E_a/RT + \ln f(\alpha)$$

or

$$\ln\alpha' - \ln f(\alpha) = \ln(A/\beta) - E_a/RT \quad (4)$$

**Results and Discussion.** – *Magnetic Susceptibility.* All the complexes **1**–**7** studied present very low values for the magnetic moments (0.11–0.00 B.M.), as it is the case in similar $W^V$ complexes [7–14]. This can be attributed to an interaction through the bridge atoms or to the possible formation of a direct metal–metal bond, as has been established for similar $[Mo^V(oxo)]$ complexes [33–35].

*Infrared Spectra.* The IR spectra show, in all cases, a band in the range 540–501 $cm^{-1}$, which was attributed to the vibration of the terminal W=S bond (*Table 2*). If we compare the parent complex **1** with the adducts $[W_2B_2(pipCS_2)_2S_2(\mu\text{-}S)_2]$ **2**–**7**, one observes that the adducts have the W=S band displaced to lower frequencies (from 540 to 528–501 $cm^{-1}$). This displacement can be attributed to the different basicity of the pyridine or substituted-pyridine ligand employed. The $pK_b$ value reflects the basicity of the ligand towards the proton. It may be assumed that the $pK_b$ of the ligand B provides a measure of the ligand ability to form $\sigma$-bonds to metal ions. In general, the higher the basicity is, the lower is the frequency of the W=S vibration.

Table 2. *Infrared Absorption Maxima* ($\tilde{\nu}$ in $cm^{-1}$) *of S-Coordinated* $W^V$ *Complexes.* $S_b$ = Bridging S-ligand.

| | $\tilde{\nu}$(W=S) | $\tilde{\nu}_a$(W–$S_b$) | $\tilde{\nu}_s$(W–$S_b$) | $\tilde{\nu}$(C–N) | $\tilde{\nu}$(C–S) | $\tilde{\nu}$(W–N) | $pK_b$(B) |
|---|---|---|---|---|---|---|---|
| **1** $[W_2(pipCS_2)_2S_2(\mu\text{-}S)_2]$ | 540 | 463 | 370 | 1520 | 1105 | – | – |
| **2** $[W_2(pipCS_2)_2(py)_2S_2(\mu\text{-}S)_2]$ | 528 | 462 | 368 | 1518 | 1099 | 340 | 8.87 |
| **3** $[W_2(pipCS_2)_2(3\text{-}Mepy)_2S_2(\mu\text{-}S)_2]$ | 524 | 460 | 366 | 1515 | 1095 | 343 | 8.32 |
| **4** $[W_2(pipCS_2)_2(4\text{-}Mepy)_2S_2(\mu\text{-}S)_2]$ | 522 | 455 | 360 | 1514 | 1085 | 345 | 7.98 |
| **5** $[W_2(pipCS_2)_2(3,5\text{-}Me_2py)_2S_2(\mu\text{-}S)_2]$ | 520 | 457 | 362 | 1510 | 1087 | 346 | 7.85 |
| **6** $[W_2(pipCS_2)_2(3\text{-}pyNH_2)_2S_2(\mu\text{-}S)_2]$ | 517 | 461 | 364 | 1512 | 1088 | 348 | 7.49 |
| **7** $[W_2(pipCS_2)_2(4\text{-}pyNH_2)_2S_2(\mu\text{-}S)_2]$ | 501 | 460 | 368 | 1511 | 1080 | 356 | 4.88 |

The IR spectra of the adducts exhibit a band in the region 356–340 $cm^{-1}$, which is assigned to the stretching vibration of the W–N(base) bond [36–38]. The order of the adducts, listed by decreasing frequencies of this band, is **7** > **6** > **5** > **4** > **3** > **2**. These

differences can be attributed to the electron donation of the pyridine or substituted-pyridine ligand to the W-atom (N → W) which increases the electron density in the metal d-orbitals, and consequently, the $p_\pi \rightarrow d_\pi$ donation from the S-atom to the W-atom is expected to be reduced to an extent which depends on the donor ability of the base. As a result, there will be a lowering of the W=S bond (hence, $\tilde{\nu}$(W=S)) and a higher frequency of the W–N bond.

We assign the bands corresponding to the W–S–W bridge ($S_b$ = bridging S), which appear at 463–455 and 370–360 $cm^{-1}$, to the antisymmetric and symmetric stretching mode, respectively. Finally, the C–N and C–S vibrations appear at 1520–1510 and 1105–1080 $cm^{-1}$, respectively. The displacement to higher frequencies for the C–N band and to lower frequencies for the C–S band, in comparison with sodium carbamodithioate, are indicative of bidentate ligands [39].

*UV/VIS Spectra.* The electronic spectra (*Table 3*) of the complexes **1**–**7** are in accordance with the *Ballhausen – Gray* and *Gray – Hare* schemes [40][41] for a square-pyramidal structure of complex **1** and a distorted octahedral structure for the adducts **2**–**7**.

*Fig. 1* shows the UV/VIS spectrum of the complex $[W_2(pipCS_2)_2(py)_2S_2(\mu\text{-}S)_2]$ (**2**). The electronic spectra of all the complexes **1**–**7** present a band in the 18554–16805 $cm^{-1}$ region, which can be assigned to a $^2B_2 \rightarrow {}^2B_1$ transition. This band shows the higher or lower bonding force from the W-atom to the ligand. Therefore, the band is displaced to higher frequencies in the adducts because of the introduction of the base ligand in the six-coordination position, and the '*trans*' effect strengthens the ligand–W $\sigma$-bond as observed in the IR spectra (*Table 2*).

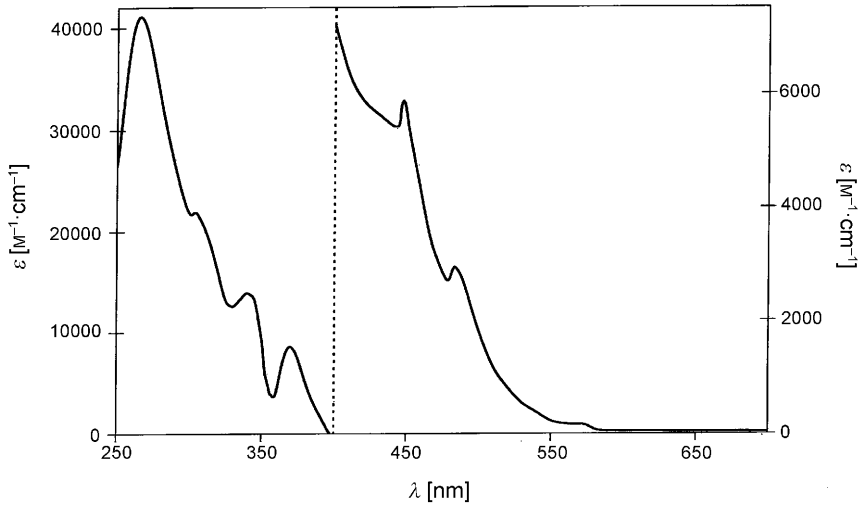


Fig. 1. *UV/VIS Spectrum of the complex* $[W_2(pipCS_2)_2(py)_2S_2(\mu\text{-}S)_2]$ (**2**)

In the VIS zone, three other bands appear at 20126–21360, 21981–22845, and 26595–27522 $cm^{-1}$, which were attributed to charge-transfer transitions. The band between 21981 and 22845 $cm^{-1}$ arises from a $S^{2-} \rightarrow W^V$ charge transfer, as observed in

Table 3. *Electronic Absorption Spectra of S-Coordinated $W^V$ Complexes*

| | $\tilde{\nu}$ [$cm^{-1}$] | $\varepsilon$ [$M^{-1} \cdot cm^{-1}$] | Transition |
|---|---|---|---|
| **1** [$W_2(pipCS_2)_2S_2(\mu\text{-}S)_2$] | 16805 | 170 | $^2B_2 \rightarrow {}^2B_1$ |
| | 20643 | 2915 | charge transfer |
| | 22738 | 5230 | charge transfer |
| | 26794 | 9185 | charge transfer |
| | 28671 | 14320 | $n \rightarrow n^*$ |
| | 33344 | 22010 | $\pi \rightarrow \pi^*$ |
| | 37879 | 40090 | $n \rightarrow \sigma^*$ |
| **2** [$W_2(pipCS_2)_2(py)_2S_2(\mu\text{-}S)_2$] | 17422 | 155 | $^2B_2 \rightarrow {}^2B_1$ |
| | 20662 | 2935 | charge transfer |
| | 22312 | 5892 | charge transfer |
| | 26595 | 9247 | charge transfer |
| | 29462 | 13925 | $n \rightarrow n^*$ |
| | 32965 | 21990 | $\pi \rightarrow \pi^*$ |
| | 37841 | 41115 | $n \rightarrow \sigma^*$ |
| **3** [$W_2(pipCS_2)_2(3\text{-}Mepy)_2S_2(\mu\text{-}S)_2$] | 17594 | 164 | $^2B_2 \rightarrow {}^2B_1$ |
| | 20613 | 3004 | charge transfer |
| | 22530 | 5933 | charge transfer |
| | 26675 | 8905 | charge transfer |
| | 29150 | 14756 | $n \rightarrow n^*$ |
| | 33005 | 22007 | $\pi \rightarrow \pi^*$ |
| | 37895 | 41576 | $n \rightarrow \sigma^*$ |
| **4** [$W_2(pipCS_2)_2(4\text{-}Mepy)_2S_2(\mu\text{-}S)_2$] | 17421 | 144 | $^2B_2 \rightarrow {}^2B_1$ |
| | 20341 | 3033 | charge transfer |
| | 21981 | 5035 | charge transfer |
| | 26845 | 7954 | charge transfer |
| | 31277 | 15733 | $n \rightarrow n^*$ |
| | 33002 | 21658 | $\pi \rightarrow \pi^*$ |
| | 37910 | 41082 | $n \rightarrow \sigma^*$ |
| **5** [$W_2(pipCS_2)_2(3,5\text{-}Me_2py)_2S_2(\mu\text{-}S)_2$] | 17810 | 240 | $^2B_2 \rightarrow {}^2B_1$ |
| | 21360 | 2227 | charge transfer |
| | 22545 | 3465 | charge transfer |
| | 26996 | 8095 | charge transfer |
| | 29358 | 17125 | $n \rightarrow n^*$ |
| | 32560 | 23074 | $\pi \rightarrow \pi^*$ |
| | 36854 | 36532 | $n \rightarrow \sigma^*$ |
| **6** [$W_2(pipCS_2)_2(3\text{-}pyNH_2)_2S_2(\mu\text{-}S)_2$] | 18021 | 215 | $^2B_2 \rightarrow {}^2B_1$ |
| | 21326 | 2327 | charge transfer |
| | 22215 | 3544 | charge transfer |
| | 27522 | 7210 | charge transfer |
| | 30657 | 14485 | $n \rightarrow n^*$ |
| | 32645 | 20207 | $\pi \rightarrow \pi^*$ |
| | 36044 | 32478 | $n \rightarrow \sigma^*$ |
| **7** [$W_2(pipCS_2)_2(4\text{-}pyNH_2)_2S_2(\mu\text{-}S)_2$] | 18554 | 254 | $^2B_2 \rightarrow {}^2B_1$ |
| | 20126 | 2208 | charge transfer |
| | 22845 | 4017 | charge transfer |
| | 27003 | 6414 | charge transfer |
| | 31728 | 14129 | $n \rightarrow n^*$ |
| | 32980 | 22377 | $\pi \rightarrow \pi^*$ |
| | 35985 | 34006 | $n \rightarrow \sigma^*$ |

other transition-metal complexes with S-bridging ligands [42][1]. In the UV zone, three transitions are detected at *ca.* 29000–31000, *ca.* 33000, and *ca.* 36000–38000 $cm^{-1}$, which are attributable to intraligand transitions like $n \rightarrow n^*$, $\pi \rightarrow \pi^*$, and $n \rightarrow \sigma^*$, respectively.

*Differential-Scanning Calorimetry* (DSC), *Thermogravimetry* (TG), *and Kinetic Studies.* The DSC curves of all complexes **2**–**7** show the first endothermic peak between 120 and 187°. The mass loss accompanying this transition corresponds in the TG curves to the loss of two moles of the base coordinated to the W-atoms, the residue being $[W_2(pipCS_2)_2S_2(\mu\text{-}S)_2]$ in all cases. Afterwards, a series of exothermic processes occur between 227 and 531°, corresponding to the decomposition of the $[W_2(pipCS_2)_2S_2(\mu\text{-}S)_2]$ complex, the residue being $WO_3$. *Fig. 2* shows the DSC and TG curves of the adduct $[W_2(pipCS_2)_2(py)_2S_2(\mu\text{-}S)_2]$ (**2**), and *Table 4* summarizes the data obtained from the DSC curve, $\alpha$ being the reacted fraction at time $t$ and $\alpha' = d\alpha/dT$.

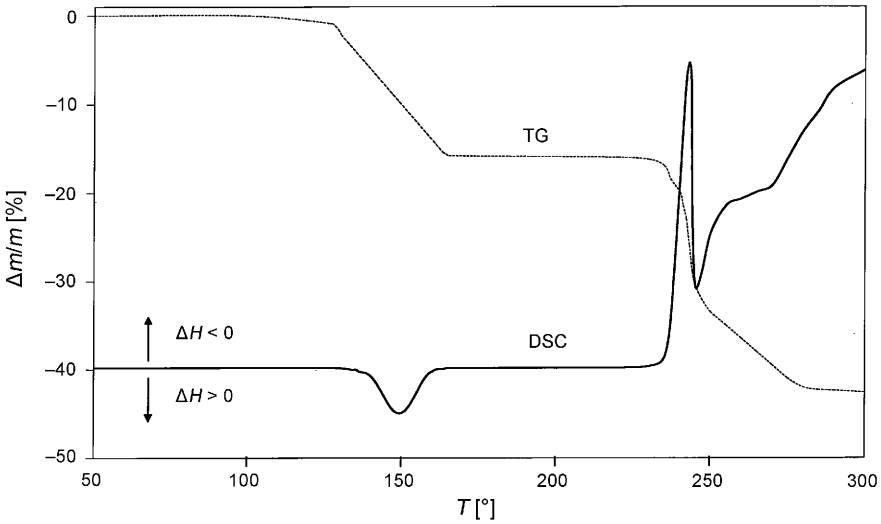


Fig. 2. *TG and DSC Curves of the complex* $[W_2(pipCS_2)_2(py)_2S_2(\mu\text{-}S)_2]$ (**2**)

We plotted $[\Delta\ln\alpha' - \Delta\ln f(\alpha)]/\Delta\ln(1-\alpha)]$ *vs.* $[\Delta(1/T)/\Delta\ln(1-\alpha)]$ (see *Eqn. 3*). From these plots, we calculated the activation energy of the process. *Table 5* shows the correlation coefficient $r$, the slope $m$, the intercept value $i$, and the activation energy $E_a$ obtained for seven different mechanisms. In all cases, the correlation coefficients $r$ are very near to unity, which is consistent with the results of *Criado et al.* [43]. Nevertheless, only when the analysis was performed with the mechanisms $D3$ and $R2$, the straight line presents an intercept value $i$ close to zero.

To test the validity of the above results and determine the mechanism, we substituted the seven forms of $f(\alpha)$ into the *Arrhenius* equation in logarithmic form, giving the equation $\ln\alpha' - \ln f(\alpha) = \ln(A/\beta) - E_a/RT$, and represented the plot of $\ln\alpha' - \ln f(\alpha)$ *vs.* $1/T$ (see *Eqn. 4*). This plot should be a straight line with a slope of $-E_a/R$ and an intercept value of $\ln(A/\beta)$. If the proposed mechanism were correct ($D3$ or $R2$), the

Table 4. *ΔH, α,* T, *and α′ Obtained from the DSC Curve of the Complex [$W_2(pipCS_2)_2(py)_2S_2(\mu\text{-}S)_2$]* (**2**)

| $\Delta H$ [mJ] | $\alpha$ | $T$ [°] | $\alpha'$ [$K^{-1}$] |
|---|---|---|---|
| 253.24 | 0.10227 | 129.0 | 0.02770 |
| 280.27 | 0.11319 | 130.0 | 0.03000 |
| 311.77 | 0.12591 | 131.0 | 0.03223 |
| 343.92 | 0.13889 | 132.0 | 0.03487 |
| 379.13 | 0.15311 | 133.0 | 0.03765 |
| 416.39 | 0.16816 | 134.0 | 0.04071 |
| 457.18 | 0.18463 | 135.0 | 0.04390 |
| 500.02 | 0.20193 | 136.0 | 0.04742 |
| 546.38 | 0.22065 | 137.0 | 0.05110 |
| 595.25 | 0.24039 | 138.0 | 0.05508 |
| 649.05 | 0.26212 | 139.0 | 0.05908 |
| 704.43 | 0.28448 | 140.0 | 0.06349 |
| 765.89 | 0.30930 | 141.0 | 0.06776 |
| 828.47 | 0.33457 | 142.0 | 0.07249 |
| 897.13 | 0.36230 | 143.0 | 0.07700 |
| 967.84 | 0.39086 | 144.0 | 0.08178 |
| 1044.40 | 0.42177 | 145.0 | 0.08625 |
| 1121.60 | 0.45296 | 146.0 | 0.09104 |
| 1205.60 | 0.48688 | 147.0 | 0.09517 |
| 1289.30 | 0.52068 | 148.0 | 0.09954 |
| 1380.70 | 0.55761 | 149.0 | 0.10274 |
| 1470.50 | 0.59385 | 150.0 | 0.10605 |
| 1567.50 | 0.63303 | 151.0 | 0.10771 |
| 1662.80 | 0.67153 | 152.0 | 0.10896 |
| 1764.90 | 0.71276 | 153.0 | 0.10783 |
| 1863.50 | 0.75258 | 154.0 | 0.10585 |
| 1968.00 | 0.79475 | 155.0 | 0.10050 |
| 2066.50 | 0.83456 | 156.0 | 0.09369 |
| 2167.70 | 0.87542 | 157.0 | 0.08258 |

Table 5. *Results Obtained by Using the Seven Mechanisms for the Plot of [$\Delta\ln\alpha' - \Delta\ln f(\alpha)$]/[$\Delta\ln(1-\alpha)$]* vs. *[$\Delta(1/T)/\Delta\ln(1-\alpha)$] for the Complex [$W_2(pipCS_2)_2(py)_2S_2(\mu\text{-}S)_2$]* (**2**)

| Mechanism | $r$ | $m$ | $i$ | $E_a$ [kJ · $mol^{-1}$] |
|---|---|---|---|---|
| *D*1 | – 0.99984 | – 31178.70 | 0.92872 | 259.2 ± 0.3 |
| *D*2 | – 0.99972 | – 31414.41 | 0.52079 | 261.2 ± 0.5 |
| *D*3 | – 0.99999 | – 31387.37 | 0.01030 | 260.9 ± 0.2 |
| *D*4 | – 0.99981 | – 31387.36 | 0.34363 | 261.0 ± 0.3 |
| *F*1 | – 0.99732 | – 14226.34 | – 0.44040 | 118.3 ± 0.3 |
| *R*2 | – 0.99730 | – 14226.33 | 0.05960 | 118.3 ± 0.1 |
| *R*3 | – 0.99732 | – 14226.33 | – 0.10706 | 118.2 ± 0.3 |

activation energy should be the same as that obtained previously. The values of the activation energy obtained for both analyses for the complex [$W_2(pipCS_2)_2(py)_2S_2(\mu\text{-}S)_2$] (**2**) show that only the mechanism *D*3 exhibits a very good agreement, with a difference of 0.31% between both values of the activation energy (*Table 6*). Therefore, in accord with our proposed method, we deduce that the thermal decomposition of **2**

Table 6. *Activation Energy Values* $E_a$ *for the Seven Mechanism Applied to the Complex* $[W_2(pipCS_2)_2(py)_2S_2(\mu\text{-}S)_2]$ (**2**)

| Mechanism | $E_a$[a]) [kJ · mol$^{-1}$] | $E_a$[b]) [kJ · mol$^{-1}$] | Difference [%] |
|---|---|---|---|
| *D*1 | 259.2 ± 0.3 | 181.3 ± 0.4 | 30.05 |
| *D*2 | 261.2 ± 0.5 | 217.5 ± 0.9 | 16.73 |
| *D*3 | 260.9 ± 0.2 | 260.1 ± 0.6 | 0.31 |
| *D*4 | 261.0 ± 0.3 | 232.2 ± 0.2 | 11.03 |
| *F*1 | 118.3 ± 0.3 | 154.5 ± 0.5 | 30.60 |
| *R*2 | 118.3 ± 0.1 | 112.5 ± 0.6 | 4.90 |
| *R*3 | 118.2 ± 0.3 | 126.5 ± 0.3 | 7.02 |

[a]) Calculated from our proposed method. [b]) Calculated from the *Arrhenius* equation.

and the loss of pyridine occurs by a *D*3 mechanism (three-dimensional diffusion: *Jander*'s equation) with a function $(3/2)(1-\alpha)^{2/3}[1-(1-\alpha)^{1/3}]^{-1}$, an activation energy $E_a = 260.9 \pm 0.2$ kJ/mol, and a pre-exponential *Arrhenius* factor $A = (1.4 \pm 0.1) \cdot 10^{29}$ s$^{-1}$. We can assume that the thermal decomposition and the loss of the coordinated base of the adducts **3**–**7** with 3-methylpyridine, 4-methylpyridine, 3,5-dimethylpyridine, pyridin-3-amine, and pyridin-4-amine, respectively, also follow a *D*3 mechanism.

*Table 7* summarizes the thermal and kinetic parameters for all complexes **2**–**7**. The results show that the higher the basicity of the base B, the higher is the activation energy $E_a$ and the pre-exponential *Arrhenius* factor *A* for the process of the loss of the base B, except for the adduct **7** with 4-pyNH$_2$. This exception can be attributed to the existence of resonance structures and their pronounced effect on the stability of the complex [31][44][45]. The data in *Table 7* also establish that the steric hindrance of the base 3,5-Me$_2$py does not modify the kinetic parameters. The plot of p$K_b$ *vs.* $E_a$ in *Fig. 3* shows a

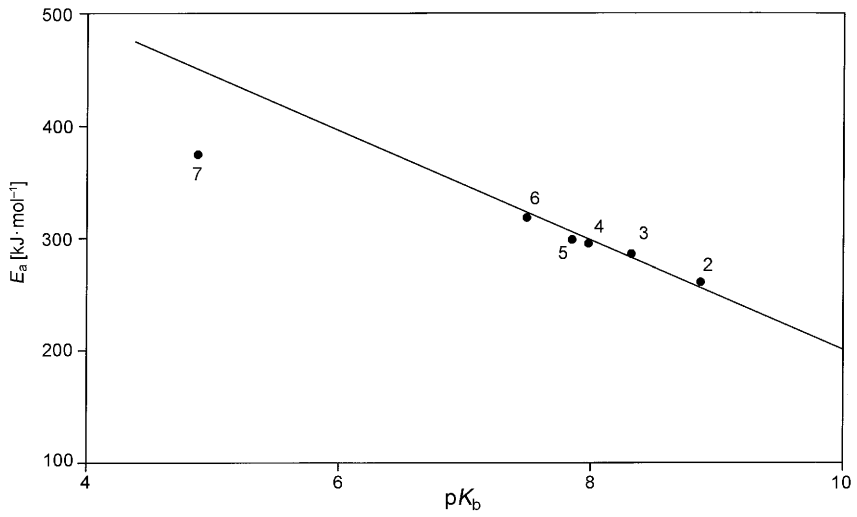


Fig. 3. *Activation energy for the decomposition of the* $[W_2B_2(pipCS_2)_2S_2(\mu\text{-}S)_2]$ *complexes* **2**–**7** vs. $pK_b$. B: py in **2**, 3-Mepy in **3**, 4-Mepy in **4**, 3,5-Me$_2$py in **5**, 3-pyNH$_2$ in **6**, and 4-pyNH$_2$ in **7**.

Table 7. *Thermal and Kinetic Parameters for the Complexes [$W_2B_2(pipCS_2)_2S_2(\mu\text{-}S)_2$]* **2**–**7**

| | Mechanism | $\Delta H$ [kJ·mol$^{-1}$] | $E_a$ [kJ·mol$^{-1}$] | $A$ [s$^{-1}$] | p$K_b$ (B) |
|---|---|---|---|---|---|
| **2** [$W_2(pipCS_2)_2(py)_2S_2(\mu\text{-}S)_2$] | *D*3 | 42.4 ± 0.6 | 260.9 ± 0.2 | $(1.4 \pm 0.1) \cdot 10^{29}$ | 8.87 |
| **3** [$W_2(pipCS_2)_2(3\text{-}Mepy)_2S_2(\mu\text{-}S)_2$] | *D*3 | 68.5 ± 0.3 | 285.9 ± 0.5 | $(2.6 \pm 0.2) \cdot 10^{30}$ | 8.32 |
| **4** [$W_2(pipCS_2)_2(4\text{-}Mepy)_2S_2(\mu\text{-}S)_2$] | *D*3 | 83.0 ± 0.7 | 295.3 ± 0.1 | $(5.9 \pm 0.5) \cdot 10^{28}$ | 7.98 |
| **5** [$W_2(pipCS_2)_2(3,5\text{-}Me_2py)_2S_2(\mu\text{-}S)_2$] | *D*3 | 91.4 ± 0.4 | 298.7 ± 0.5 | $(8.0 \pm 0.4) \cdot 10^{30}$ | 7.85 |
| **6** [$W_2(pipCS_2)_2(3\text{-}pyNH_2)_2S_2(\mu\text{-}S)_2$] | *D*3 | 107.6 ± 0.6 | 318.3 ± 0.6 | $(6.4 \pm 0.2) \cdot 10^{31}$ | 7.49 |
| **7** [$W_2(pipCS_2)_2(4\text{-}pyNH_2)_2S_2(\mu\text{-}S)_2$] | *D*3 | 193.3 ± 0.8 | 374.7 ± 0.7 | $(9.1 \pm 0.6) \cdot 10^{30}$ | 4.88 |

very satisfactory correlation, except for the 4-pyNH$_2$ adduct **7**, and confirms that the activation energy is linearly related to the basicity of the ligands.

## REFERENCES


[1] A. Kay, P. C. H. Mitchell, *J. Chem. Soc. A* **1970**, 2421.
[2] F. A. Cotton, D. L. Hunter, R. Weiss, *J. Coord. Chem.* **1974**, *3*, 259.
[3] F. A. Schultz, V. R. Ott, D. S. Rolison, D. C. Braward, J. W. McDonald, W. E. Newton, *Inorg. Chem.* **1978**, *17*, 1758.
[4] R. Lozano, A. L. Doadrio, A. Doadrio, *Polyhedron* **1982**, *1*, 163.
[5] R. Lozano, J. Román, E. Alarcón, A. L. Doadrio, A. Doadrio, *Rev. Chim. Minér.* **1983**, *20*, 173.
[6] R. Lozano, J. Román, M. D. Armada, A. Doadrio, *Polyhedron* **1985**, *4*, 1563.
[7] R. Lozano, A. L. Doadrio, E. Alarcón, J. Román, A. Doadrio, *Rev. Chim. Minér.* **1983**, *20*, 109.
[8] R. Lozano, E. Alarcón, A. L. Doadrio, A. Doadrio, *Polyhedron* **1983**, *2*, 435.
[9] R. Lozano, E. Alarcón, A. L. Doadrio, A. Doadrio, *Polyhedron* **1984**, *3*, 25.
[10] R. Lozano, E. Alarcón, J. Román, A. Doadrio, *Rev. Chim. Minér.* **1984**, *21*, 177.
[11] R. Lozano, E. Alarcón, J. Román, A. Doadrio, *Polyhedron* **1984**, *3*, 1021.
[12] R. Lozano, J. Román, M. D. Armada, E. Parrondo, *Eur. J. Solid State Inorg. Chem.* **1988**, *25*, 191.
[13] R. Lozano, J. Román, F. de Jesús, *Polyhedron* **1989**, *8*, 947.
[14] R. Lozano, F. de Jesús, M. C. Lozano, *Polyhedron* **2006**, *25*, 3127.
[15] E. I. Stiefel, *Prog. Inorg. Chem.* **1977**, *1*, 22.
[16] B. K. Burgess, D. B. Jacobs, E. I. Stiefel, *Biochim. Biophys. Acta*, *Enzymol.* **1980**, *614*, 196.
[17] C. Sharp, A. G. Sykes, *Inorg. Chem.* **1988**, *27*, 501.
[18] M. R. Maurya, N. Bharti, *Transition Met. Chem.* **1999**, *24*, 389.
[19] K. Umakoshi, E. Nishimoto, M. Sokolov, H. Kawano, Y. Sasaki, M. Onishi, *J. Organomet. Chem.* **2000**, *611*, 370.
[20] B. Keshavan, K. Gowda, *Proc. Indian Acad. Sci.* **2001**, *3*, 165.
[21] E. S. Freeman, B. Carroll, *J. Phys. Chem.* **1958**, *62*, 394.
[22] A. E. Nerwkirk, *Anal. Chem.* **1960**, *32*, 1558.
[23] C. D. Doyle, *J. Appl. Polym. Sci.* **1961**, *5*, 285.
[24] H. H. Horowitz, G. Metzger, *Anal. Chem.* **1963**, *35*, 1464.
[25] A. W. Coats, J. P. Redfern, *Nature (London, U.K.)* **1964**, *201*, 68.
[26] J. M. Thomas, T. A. Clarke, *J. Chem. Soc. A* **1968**, 457.
[27] W. W. Wendlant, 'Thermal Methods of Analysis', Wiley, New York, 1974.
[28] T. R. Ingraham, P. Marrier, *Can. J. Chem. Eng.* **1984**, 161.
[29] R. Lozano, J. Román, F. de Jesús, A. Jerez, M. Gaitán, E. Ramos, *Thermochim. Acta* **1989**, *141*, 261.
[30] R. Lozano, J. Román, F. de Jesús, A. Jerez, M. Gaitán, E. Ramos, *Thermochim. Acta* **1989**, *143*, 93.
[31] R. Lozano, J. Martínez, A. Martínez, J. Román, F. de Jesús, *Polyhedron* **1989**, *8*, 2611.
[32] P. W. Selwood, 'Magnetochemistry', Interscience, New York, 1956.
[33] F. A. Cotton, S. M. Morehouse, J. S. Wood, *Inorg. Chem.* **1964**, *3*, 1063.
[34] L. Ricard, C. Martin, R. Wiest, R. Weiss, *Inorg. Chem.* **1975**, *14*, 2300.

[35] L. Ricard, J. Stienne, J. Karagiannidis, P. Toledano, J. Fisher, A. Mitschler, *J. Coord. Chem.* **1974**, *3*, 277.
[36] M. H. Chisholm, J. C. Huffman, J. W. Pasterczyk, *Polyhedron* **1987**, *6*, 551.
[37] M. A. Ansari, J. Chandrasekaran, S. Sarkar, *Polyhedron* **1988**, *7*, 471.
[38] V. C. Gibson, T. P. Kee, A. Shaw, *Polyhedron* **1988**, *7*, 579.
[39] A. Doadrio, A. L. Doadrio, *An. Quim.* **1977**, *73*, 959.
[40] C. J. Ballhausen, H. B., Gray, 'Molecular Orbital Theory', Benjamin, New York, 1965.
[41] H. B. Gray, C. R. Hare, *Inorg. Chem.* **1962**, *1*, 363.
[42] I. G. Dance, A. E. Landers, *Inorg. Chem.* **1979**, *18*, 3487.
[43] J. M. Criado, D. Dollimore, G. R. Heal, *Thermochim. Acta* **1982**, *54*, 159.
[44] R. Lozano, J. Martínez, A. Martínez, A. Doadrio, *Polyhedron* **1983**, *2*, 997.
[45] R. Lozano, J. Román, J. Martínez, A. Martínez, A. Doadrio, *Polyhedron* **1986**, *5*, 1341.

*Received March 31, 2008*